28300

Summary of Results and Conclusions Based on Analysis of Volume Imaging and High Spectral Resolution Lidar Data Acquired During FIRE Phase I: Part II

C. J. Grund and **E. W. Eloranta**
University of Wisconsin
Department of Meteorology
1225 West Dayton St.
Madison, WI 53706

NOTE: *Continuation from part I... see Grund and Eloranta in oral presentation section.*

IV. Summary

Since the fall of 1986, we have observed cirrus clouds with backscatter cross sections ranging from $<1 \cdot 10^{-7}$ - $4.2 \cdot 10^{-5}$ m^{-1} sr^{-1}, optical thicknesses ranging from <.003 to >2.7 , and bulk average backscatter phase functions from .02 - .065 sr^{-1}. We have recorded cirrus cloud structures ranging in vertical extent from 0.1 to 8 km, having horizontal scales from 10's of meters to 266 km, and exhibiting aspect ratios of from 1:5 to 1:100.

The altitude relationship between cloud top and bottom boundaries and the optical center of the cloud is influenced by the type of formation observed. Altocumulus and uncinus generating regions tend to concentrate attenuation in regions of less than 200 m thickness which dominate the vertical extinction profile, even when the generating cell caps an extended column of virga. Virga exhibits complicated fine scale structure, often lying in interleaved, sheared sheets. In cirrostratus, imbedded vertically developed cells frequently occupy a significant altitude range and create large spatial inhomogeneities in optical properties.

Cirrus morphology and generation processes appear to be related to the wind field. Better temporal and spatial resolution in wind measurements in future experiments would aid the understanding of cirrus generation and dissipation mechanisms.

The characterization of the microphysical, morphological and optical properties on satellite footprint and model grid sized areas could be improved in future experiments by characterizing the 3D volume in which the insitu measurements are acquired. High spatial resolution characterization of the distribution of cirrus could be profitably used to shed light on the relationship between aircraft measurements and cirrus formations.

The HSRL has been successfully adapted to the task of cirrus cloud optical property measurement. The HSRL data reported here were collected with the $CuCl_2$ transmitter producing 50 mW of output power, achieving eye-safe, direct optical depth and backscatter cross section measurements with 10 minute averaging times. A continuously pumped, injection seeded, doubled Nd:YAG laser has just been installed and has increased temporal resolution by a factor of ~20, while improving the aerosol-molecular signal separation capabilities and wavelength stability of the instrument. We expect considerable further improvements as we fine tune the system.

We are just beginning a several week long field experiment in which the VIL will be operated from a site just west of Madison while the HSRL produces vertical optical property measurements. By scanning the VIL in two approximately cross wind planes, we expect to deduce high resolution winds when cirrus are present (by a time lag structural correlation technique), and to characterize the 3D context for cirrus optical properties deduced from HSRL measurements. We will be launching radiosondes in support of this effort. Satellite data acquired by Don Wylie will be subsequently used to

compare passive retrievals to the HSRL optical properties and the VIL contextual information.

Acknowledgements

Funding for VIL construction was provided under ARO grant DAAG29-84-G-0028. HSRL and VIL instrument development and data analysis with regard to cloud statistics has been supported under ARO grant DAAG29-84-K-0069 and ONR contract N00014-87-K-0436. Support for the development of VIL wind measurement capabilities has been provided under ARO grant DAAL03-86-K-0024. Recent algorithm development, and studies of the correlation between wind and backscatter are supported under AFGL contract F19628-87-0056.

References

1. Grund, C.J., and E.W. Eloranta 1989: The 27-28 October 1986 FIRE IFO cirrus cloud study: Cloud optical properties determined by the High Spectral Resolution Lidar. *Mon.Wea.Rev.* **117**, in review.
2. Grund. C.J., E.W. Eloranta, and D.P. Wylie 1989: Lidar validation of VAS Cirrus Cloud Height Determinations. 27th Aerospace Sciences Meeting Jan. 9-12, Reno, NV. *AIAA pub.* **89-0804**.
3. Sassen, K., D.O'C. Starr, and A.J. Heymsfield, 1989: The 27-28 October 1986 FIRE IFO cirrus cloud study: An experiment summary. *Mon.Wea.Rev.* **117**, in review.
4. Sassen, K., C.J. Grund, J.M. Spinhirne, M.J. Hardesty, and J.M. Alvarez 1989: The 27-28 October 1986 FIRE IFO cirrus cloud study: A five lidar overview of cloud structure and evolution. *Mon.Wea.Rev.* **117**, in review.
5. Starr, D.O'C. , and D.P. Wylie 1989: The 27-28 October 1986 FIRE IFO cirrus cloud study: Meteorology and clouds. *Mon.Wea.Rev.* **117**, in review.

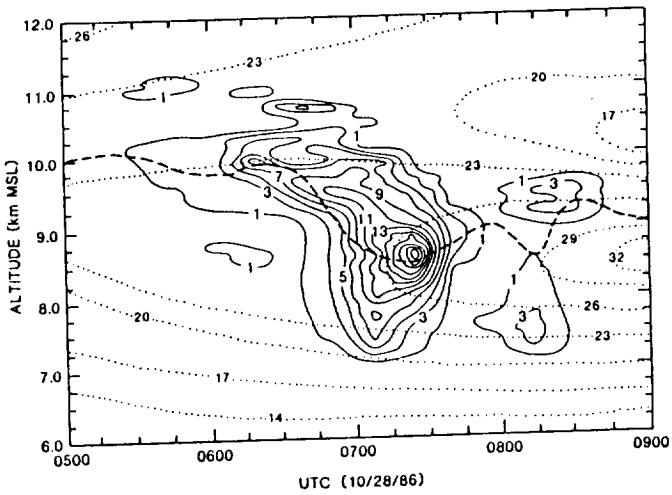

Fig. 3 Mesoscale uncinus complex. Average optical thickness between 0600 and 0750 was .58 (minimum .09 at 0750, maximum 1.1 at 0718), bulk backscatter phase function .042 sr^{-1}. Backscatter cross section (——) in 10^{-6} m^{-1} sr^{-1}, optical mid-cloud altitude (- - -), wind speed (· · ·) in m/s. The MUC passed over Madison just ahead of a mesoscale wind jet.

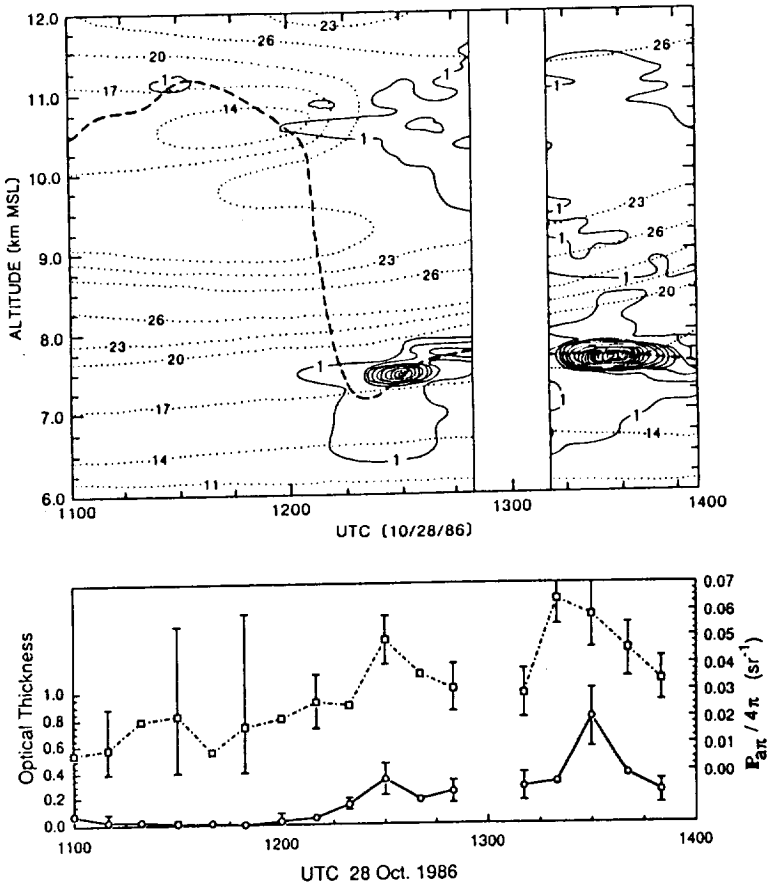

Fig. 4 (Top) Time height backscatter cross section (——,10^{-6} m^{-1} sr^{-1}, interval: 7 ·10^{-6} m^{-1} sr^{-1}) mapping of an Altocumulus - cirrus formation with isotachs (· · ·, in m/s) and optical mid-cloud altitude (- - -). Fig. 5 (Bottom) Corresponding cloud optical depth (——) and normalized bulk backscatter phase function (-·-,sr^{-1}). Note peaks in backscatter phase function coincide with ACu.

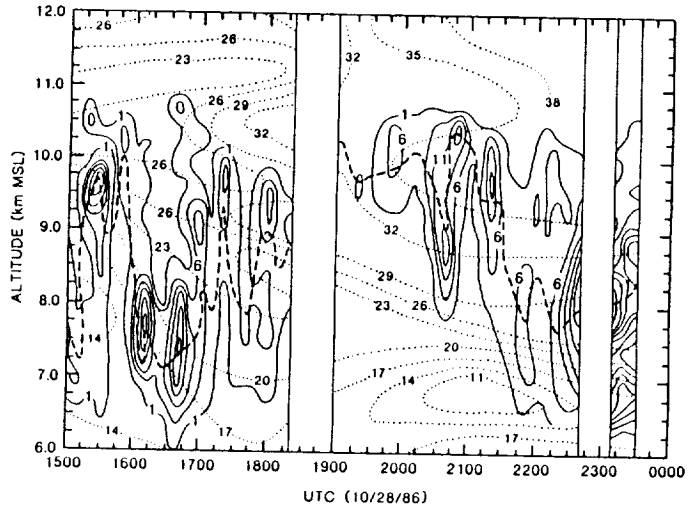

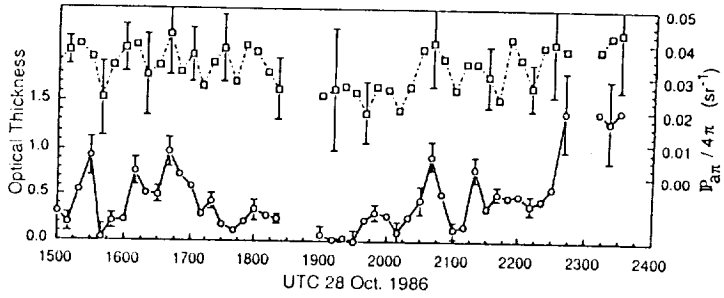

Fig. 6 (Top) Time height backscatter cross section (——, 10^{-6} m^{-1} sr^{-1}) mapping of an cirrostratus formation with isotachs (· · ·, in m/s). Optical mid-cloud altitude (- - -) tends to follow regions of intensified backscatter independent of cloud top and bottom altitudes. **Fig. 7** (Bottom) Corresponding cloud optical depth (——) and normalized bulk backscatter phase function (- - -, sr^{-1}).

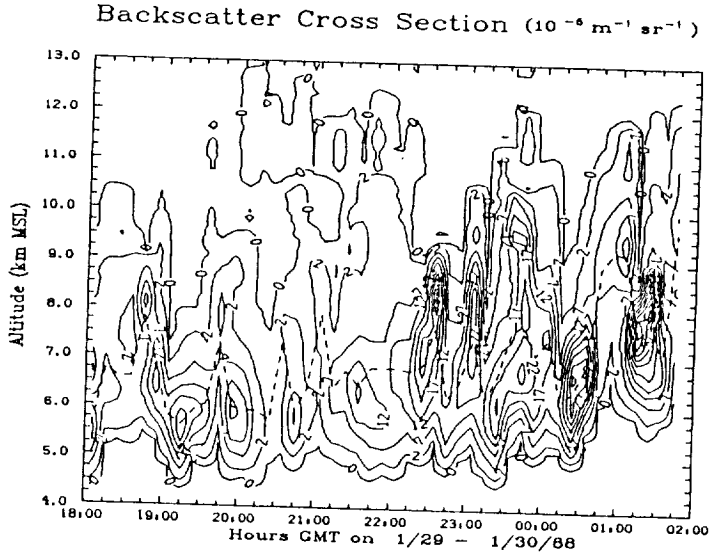

Fig. 8 Time height backscatter cross section (——, 10^{-6} m^{-1} sr^{-1}, 0 = 5.10^{-7} m^{-1} sr^{-1}) mapping of an cirrostratus formation with isotachs (· · ·, in m/s) and optical mid-cloud altitude (- - -). Repeated overlapping cell structure is inclined ~ 7° from horizontal.